IEEE Access
Multidisciplinary | Rapid Review | Open Access Journal

Received January 30, 2022, accepted February 12, 2022, date of publication February 15, 2022, date of current version February 28, 2022.

Digital Object Identifier 10.1109/ACCESS.2022.3151968

Permanent Magnet Vernier Machines for Direct-Drive Offshore Wind Power: Benefits and Challenges

DILEEP KUMAR KANA PADINHARU[1], GUANG-JIN LI[1], (Senior Member, IEEE), ZI-QIANG ZHU[1], (Fellow, IEEE), RICHARD CLARK[2], ARWYN THOMAS[2], ZIAD AZAR[2], AND ALEXANDER DUKE[2]

[1]Department of Electronic and Electrical Engineering, The University of Sheffield, Sheffield S10 2TN, U.K.
[2]Siemens Gamesa Renewable Energy Ltd., Sheffield S3 7HQ, U.K.

Corresponding author: Guang-Jin Li (g.li@sheffield.ac.uk)

This work was supported in part by the UK EPSRC Prosperity Partnership "A New Partnership in Offshore Wind" under Grant EP/R004900/1.

ABSTRACT Permanent magnet Vernier (PM-V) machines, at low power levels (few kWs), have shown a great potential to improve the torque density of existing direct-drive PM machines without much compromising on efficiency or making the machine structure more complicated. An improved torque density is very desirable for offshore wind power applications where the size of the direct-drive machine is an increasing concern. However, the relatively poor power factors of the PM-V machines will increase the power converter rating and hence cost. The objective of this paper is to review the benefits and challenges of PM-V machines for direct-drive offshore wind power applications. The review has been presented considering the system-level (direct-drive generator + converter) performance comparison between the surface-mounted permanent magnet Vernier (SPM-V) machines and the conventional SPM machines. It includes the indepth discussion on the challenges facing the PM-V machines when they are scaled up for multi-MW offshore wind power application. Other PM-V topologies discussed in literature have also been reviewed to asses their suitability for offshore wind power application.

INDEX TERMS Direct-drive wind generator, power factor, system-level performance, Vernier machine.

I. INTRODUCTION

The offshore wind market is growing rapidly with almost 24% average year-on-year growth since 2013 [1]. In 2019, the total contribution from offshore wind towards the global wind market is 10% and this number is expected to double by 2025 [1]. Most countries now see the offshore wind market as a key player to meet their renewable targets. Offshore wind technology has dramatically advanced over the past decades driving its cost down to the point that it is economically competitive against fossil-fuel alternatives [2]. One of the biggest contributors to the cost reduction is the maturity of technologies that allows building large wind turbines further out at sea [3]. Larger turbines have a larger sweep area and have access to higher and less turbulent wind, increasing their capacity factors (generate a higher proportion of their maximum potential output) [4]. Larger turbines also enable a smaller number of turbines per wind farm and thereby reducing installation time and cost. The offshore wind market has therefore shown an increasing demand for larger power ratings.

In most cases, wind turbines use a multi-stage gearbox to convert the slow turbine speed to match the synchronous speed of the generator. Currently, the studies carried out covering ∼350 offshore wind turbines indicate that the gearbox requires a replacement every 6.5 years which is much shorter than the lifespan of the turbine itself (around 20 years) [5]. The gearbox has been identified as the component contributing to the highest material cost to the offshore wind turbines due to their frequent failures and the resulting downtime [6]. Moreover, the gearbox accounts for most of the losses in the drivetrain system (∼60% for a 3MW with a 3-stage gearbox) [7]. These challenges become more significant with the increasing turbine power ratings. As an alternative,

The associate editor coordinating the review of this manuscript and approving it for publication was Kan Liu.

the direct-drive machines (turbine shaft directly coupled to the generator rotor) have become popular for offshore wind as they eliminate the requirement of the gearbox. However, the direct-drive generators are much larger in size compared to the geared counterparts because of the high torque requirement at low speed. With ever increasing turbine power ratings, these generators become bulkier, presenting new challenges like more complex logistics, increased top head mass, etc. [8], [9].

It is broadly recognized that permanent magnet (PM) synchronous machines are the most attractive candidate for direct-drive applications due to their high power density, efficiency and easy scalability [10]. Although the high cost of PM machines has been a concern, these machines can still be competitive for offshore wind farms when the long-term benefits including low operation & maintenance costs, high efficiency, simplified design and manufacturing are considered [11], [12]. With the projected rapid rise of turbine ratings going above 10MW power level, continuous effort is required to improve the torque density of these PM generators. Several solutions have been proposed in the past to improve the torque/power density of direct-drive PM machines such as transverse flux machines [13], magnetically geared machines with dual airgap [14], [15], etc. However, these machines often have complicated structures, making them less attractive for high-power applications.

Recently, Vernier machines, based on the same principle as magnetically geared machines [16], have become very popular mainly due to their high torque density combined with simple machine structure. However, these machines have a relatively low power factor compared to conventional SPM machines. Several Vernier machine topologies have been discussed in the literature to improve their torque density and power factor. However, most of the research works are largely limited to relatively small scale (up to few kWs) power levels. A few papers have been published in recent years to assess the suitability of Vernier machines for multi-MW power levels [17]–[24]. This paper aims to summarize the work published in these papers providing useful insight into the benefits and challenges of Vernier machines for direct-drive multi-MW offshore wind power applications. This involves some in-depth discussions about the following points:

- working principle and different Vernier topologies presented in literature
- impact of scaling on the system-level (direct drive generator + power converter) performance of Vernier machines in comparison with the conventional SPM machines

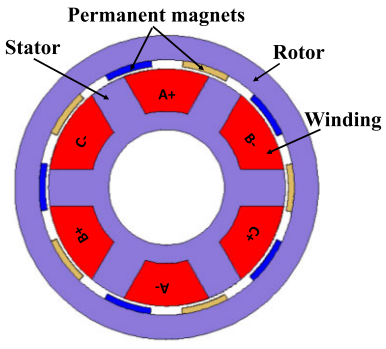

FIGURE 1. Example of an outer rotor SPM-V machine with $Z = 6$, $P_r = 5$ and $P_s = 1$.

II. BASIC PRINCIPLE OF VERNIER MACHINES

A. HIGH TORQUE DENSITY OF VERNIER MACHINES

The 2D model of a typical outer rotor surface mounted PM Vernier (SPM-V) machine with $Z = 6$, $P_r = 5$, $P_s = 1$ is shown in FIGURE 1, where Z is the number of stator slots, P_r is the number of rotor pole pairs and P_s is the number of stator winding pole pairs.

The torque-producing mechanism in Vernier machines is explained in many ways in literature. In most cases, this has been presented as follows [25]–[30]. The PM fundamental magnetomotive force (MMF) (P_r^{th} order) interacts with the airgap permeance created by the open stator slots (Z^{th} order). This generates two components in the radial airgap flux densities, i.e., one fundamental (P_r^{th} order) and one modulated [$|Z - P_r|^{\text{th}}$ and $(Z + P_r)^{\text{th}}$ order], that can contribute to the phase back electromotive force (back-EMF) and thus to the electromagnetic torque. The $|Z - P_r|^{\text{th}}$ order modulated flux density component rotates at a speed that is $P_r/(|Z - P_r|)$ times the fundamental component. This ratio of the speed of the modulated flux density to that of the fundamental component is defined as the gear ratio (G_r) of Vernier machines. A high G_r results in a high-speed modulated airgap field even for a slow-moving rotor. This phenomenon is very similar to the magnetic gearing effect. The high torque density of Vernier machines is attributed to this fast-changing modulated field component which is absent in conventional PM machines. To maximize the utilization of this high-speed low pole pair ($|Z - P_r|$) subharmonic component, the stator is wound for the same modulated pole pairs. Therefore, the slot/pole number combination of the Vernier machines follows a specific rule given by

$$P_s = |Z - P_r| \tag{1}$$

By choosing the above slot/pole number combination, one of the slot harmonic orders of the stator MMF, i.e., $[(Z/P_s) \pm 1]$, is matched with the fundamental order of the rotor PM MMF (P_r/P_s) to produce the electromagnetic torque. From (1), it can be understood that P_s can be either $(Z - P_r)$ or $(P_r - Z)$. Some early works in [31] and [32] selected the slot/pole number combinations as $P_s = P_r - Z$. However, some of the later works revealed that the harmonic coupling in the Vernier machines increased the torque when $P_s = Z - P_r$ [28]. Hence, to maximize the torque, most of the recent works in Vernier machines adopted the slot/pole number combinations as $P_s = Z - P_r$.

The high torque capability of the Vernier machines compared to the conventional surface-mounted PM (SPM)

machines is also explained by their high tangential flux density in the airgap resulting from this slot/pole number combination [33].

B. POOR POWER FACTOR OF VERNIER MACHINES

The PM-V machines are known for their high torque density but relatively poor power factor compared to the conventional SPM machines. The poor power factor of PM-V machines has been explained in literature by comparing their phasor diagram with that of a conventional SPM machine having the same stator structure [26], [30]. For the same stator structure, P_r of the PM-V machines will be G_r times higher than that of the conventional SPM machines. For example, a machine designed with $Z = 6$ and $P_s = 1$ will have $P_r = 1$ for the conventional SPM machine and $P_r = 5$ for the PM-V machine. The comparison of the phasor diagram between these two machines is shown in FIGURE 2. The inductive reactance drop in the PM-V machines, because of their higher operating frequency, is G_r times that of the conventional SPM machines. Here, the inductance between the two machines is assumed to be the same because of their similar stator structure. Whereas the induced EMF of the PM-V machines is k_c times higher than that of the conventional SPM machines. In general, $k_c \ll G_r$, and in most literature this reduced value of k_c is due to high inter-pole PM leakage fluxes. But it was revealed in [23] that the leakage fluxes due to the large coil pitch to rotor pole pitch ratio of PM-V machines are much more dominant than the inter-pole PM leakage fluxes. Overall, the PM fluxes in the PM-V machines are largely unutilized, resulting in poor power factors compared to the conventional SPM machines.

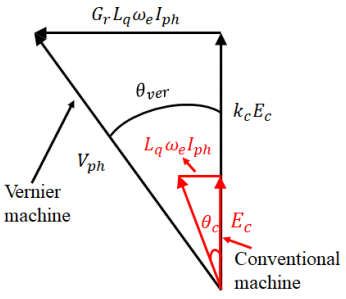

FIGURE 2. Comparison of phasor diagrams between conventional PM and PM-V machines. L_q – q-axis inductance, ω_e – angular frequency, I_{ph} – phase current, E_c – back EMF, V_{ph} – Terminal voltage, θ_c and θ_{ver} are the power factor angles for conventional SPM and Vernier machines, respectively.

C. SLOT/POLE NUMBER COMBINATIONS

To achieve higher torque density, Vernier machines are generally designed with higher G_r. Using (1), G_r can be represented in terms of slots/pole/phase (q) for a 3-phase PM-V machine as

$$fracP_rP_s = G_r = \frac{Z}{P_s} - 1 = 6q - 1 \tag{2}$$

TABLE 1. Some possible slot/pole number combinations for PM-V machines.

Z	P_r	P_s	Gear ratio (G_r)	Slot/pole/phase (q)
6	5	1	5	1
12	10	2		
9	8	1	8	1.5
18	16	2		
12	11	1	11	2
24	22	2		
15	14	1	14	2.5
30	28	2		
18	17	1	17	3
36	34	2		
21	20	1	20	3.5
42	40	2		
24	23	1	23	4
48	46	2		

To achieve higher G_r, q needs to be high and therefore Vernier machines mostly have distributed windings. Vernier machines can also be designed with fractional slot concentrated winding (FSCW) using a split teeth stator configuration which will be discussed in section section III.B. It can be understood from (2) that the minimum G_r possible for an integer slot winding, i.e. $q = 1$, is 5. Some of the possible slot/pole number combinations that satisfy (1) and with an integer gear ratio are given in TABLE 1 [30]. Their G_r and q are also highlighted.

The influence of slot/pole number combinations, G_r and q on the torque performance and power factor of the PM-V machines has been investigated through analytical models and Finite Element Analysis (FEA) [25], [26], [30]. The average torque (T_{av}) as a function of G_r, fundamental (B_{P_r}) and modulated (B_{z-P_r}) components of airgap flux density is given by [34]

$$T_{av} = \frac{\pi}{2\sqrt{2}} k_w Q \left(G_r B_{z-P_r} + B_{P_r}\right) D_g^2 L_{stk} \tag{3}$$

where k_w is the fundamental winding factor, Q is the electrical loading, D_g and L_{stk} are the airgap diameter and stack length, respectively.

Based on (3) one can conclude that the torque of the PM-V machines is proportional to G_r or q. It is worth noting that for a given G_r, the PM-V machines can be designed with different slot/pole number combinations as shown in TABLE 1. It is observed that the torque performance of the PM-V machines is better towards lower slot/pole number combinations due to lower inter-pole PM leakage fluxes [20]. However, there is an optimal G_r and slot/pole number combinaton beyond which the torque performance starts to deteriorate. This optimal torque is limited by the inter-pole PM leakage flux and the magnetic saturation [30].

The power factor, on the contrary, shows a decreasing trend with increasing G_r (assuming increased G_r is achieved by increasing P_r) [26], [30]. This is mainly due to the high inter-pole PM leakage fluxes with increasing P_r. Similiarly for a given G_r, the power factor increases towards lower slot/pole number combinations due to reduced inter-pole PM

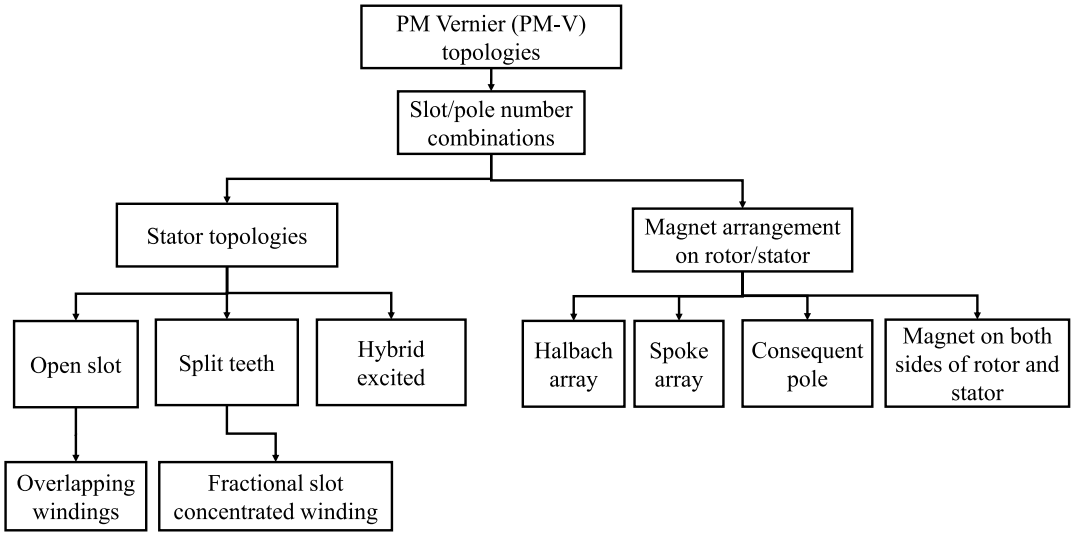

FIGURE 3. Main classifications of the PM-V topologies.

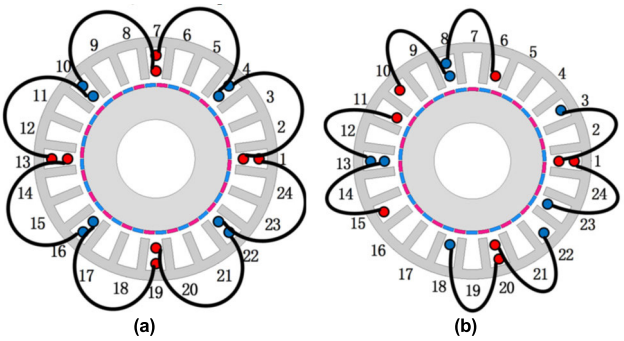

FIGURE 4. Comparison of overlapping windings with open stator slots [36]. (a) Conventional overlapping winding configuration with q ≥ 1. (b) Overlapping winding with 2-slot coil pitch.

and stator slot leakage fluxes. In summary, the performance of the PM-V machines is found to be sensitive to the slot/pole number combinations. Hence, it is important to optimize the slot/pole number combinations for overall good performance.

III. STATOR SLOT/WINDING TOPOLOGIES

In addition to the slot/pole number combinations, the stator and rotor structures with different PM arrangements on them have also been reported in literature to improve the torque density and the power factor of the PM-V machines. These are mainly classified as shown in FIGURE 3. These topologies will be discussed in detail in the following sections.

A. OPEN STATOR SLOT (OVERLAPPING WINDINGS)

As discussed before, to achieve higher torque density, the PM-V machines are generally designed with distributed stator windings. Moreover, to utilize the flux modulation effect, an open stator slot structure is preferred. Hence, the PM-V machines with an open stator slot structure and an overlapping winding topology with $q \geq 1$ have been the most commonly investigated cases [25], [26], [28], [29], [35]. A typical example of an open stator slot PM-V machine with $Z = 24, P_r = 20, P_s = 4$ ($q = 1$) is shown in FIGURE 4 (a).

Although these machines with $q \geq 1$ could achieve high torque, they have long end-windings. If the stack length of the machine is short, these end windings can considerably increase the machine volume and thereby offset the high torque density benefit.

As an attempt to reduce the end-winding length, fractional slot concentrated windings (FSCW) or non-overlapping windings are investigated for open slot PM-V machines [36]. It is observed that the maximum G_r obtained with FSCW is only 2.6. Moreover, the winding factor (k_w) is found to be inversely proportional to G_r. The investigation revealed that, as the gear ratio nears unity, the PM-V machines work as conventional FSCW PM machines and do not show any superiority. For example, a PM-V machine with $Z = 12, P_r = 7, P_s = 5$ and $G_r = 1.4$ is the same as a conventional 12s/14p FSCW PM machine [37], [38]. By comparing the PM-V machines (with open stator slots) with the conventional FSCW PM machines (with semi-closed slots), it is concluded that the PM-V machine with FSCW may not be able to improve the torque capability. Furthermore, as a tradeoff between overlapping winding with $q \geq 1$ and an FSCW, a 2-slot coil pitch overlapping winding is proposed as shown in FIGURE 4(b) [36]. The authors selected a slot/pole number combination of $Z = 24, P_r = 19, P_s = 5$ with $G_r = 3.8$. The torque capability is found to be 18% higher than the FSCW topology and 20% lower compared to the overlapping winding with $q = 1$. However, the power factor of the proposed 2-slot coil pitch design is better than that with $q = 1$ or $G_r = 5$. Hence, the proposed topology is found to be a good tradeoff between the FSCW and overlapping winding with $q \geq 1$ for reducing the end-winding length, improving the power factor but at the cost of reduced torque performance.

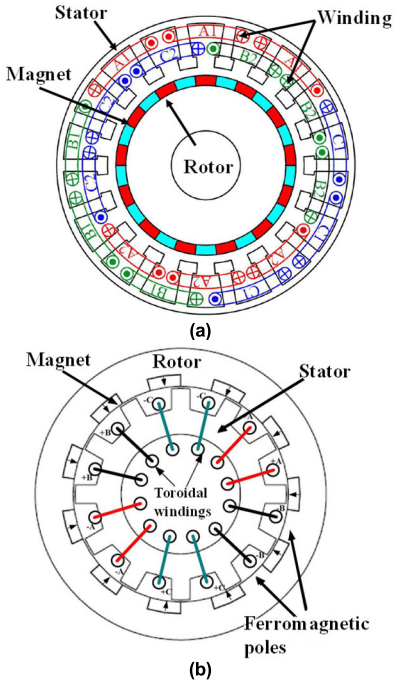

FIGURE 5. PM-V machines with different winding configurations to reduce the end winding length. (a) 2-slot coil pitch windings [39]. (b) Toroidal windings [40].

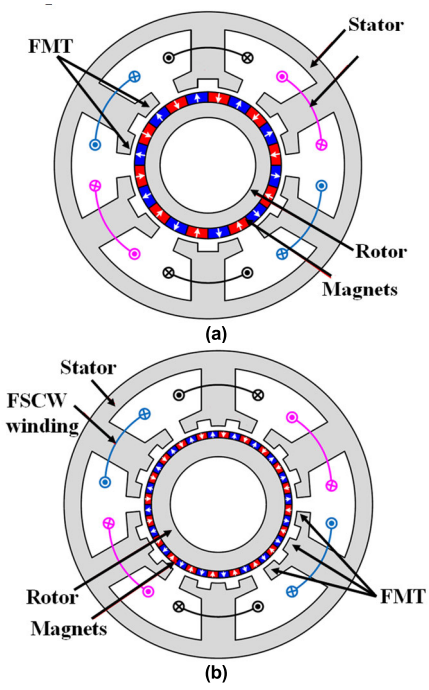

FIGURE 6. Comparison of PM-V machines with the different numbers of FMT on the split teeth stator topology [44]. (a) Split teeth stator with 2 FMT. (b) Split teeth stator with 3 FMT.

A novel 2-slot coil pitch PM-V machine with open stator slots is discussed in [39] and is shown in FIGURE 5(a). By adopting this winding arrangement, the authors claimed that the armature field harmonics and inductance can be reduced without compromising the fundamental components.

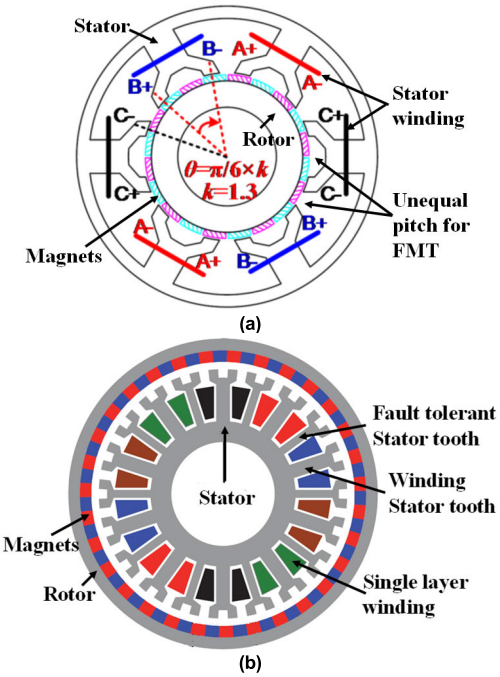

FIGURE 7. Split teeth stator PM-V machines with improved torque density and fault-tolerant capability. (a) Unequal pitch for FMT [46]. (b) Improved fault-tolerant capability [47].

This resulted in a higher power factor (0.95) with better torque and flux weakening capability.

Similarly, to reduce the end-winding length in open slot topologies, toroidal windings have also been investigated [40]–[43]. A single airgap consequent pole PM-V machine with toroidal windings as shown in FIGURE 5(b) could achieve 20% higher torque with only 66% PM usage compared to an overlapping winding PM-V machine. To improve the utilization of stator winding flux, dual airgap with dual stator [41] or dual rotor [42] topologies have also been proposed.

B. SPLIT TEETH STATOR (NON-OVERLAPPING WINDINGS)

As discussed in the previous section, the G_r achieved with open stator slot FSCW topology is very low (<3). To realize an FSCW with high G_r, the PM-V machines with split teeth stator is developed as shown in FIGURE 6.

Split teeth stator has multiple flux (field) modulating teeth (FMT) on one stator tooth, on which the armature winding is wound. This helps to have a large number of FMT for a reduced number of stator slots. This allows for an FSCW topology without compromising the high G_r. The number of FMT on one stator tooth can be increased to achieve a higher gear ratio. For example, the PM-V machine shown in FIGURE 6(a) has 2 FMT per stator tooth and G_r is 5, and hence for this machine $Z = 6, FMT = 12, P_r = 10$, and $P_s = 2$. By increasing the number of FMT to 3 per stator tooth as shown in FIGURE 6(b), but maintaining the same stator winding structure, a $G_r = 10$ can be achieved. Although the split teeth topology can increase the gear ratio,

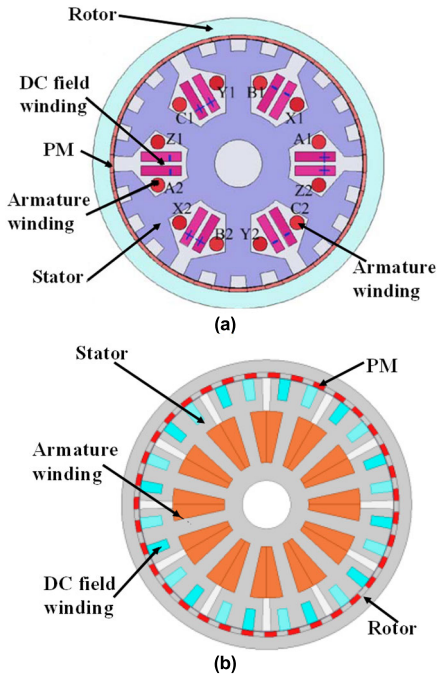

FIGURE 8. HEPM-V machine topologies. (a) Field and armature windings sharing the same slot [53]. (b) DC field windings in the FMT slots [54].

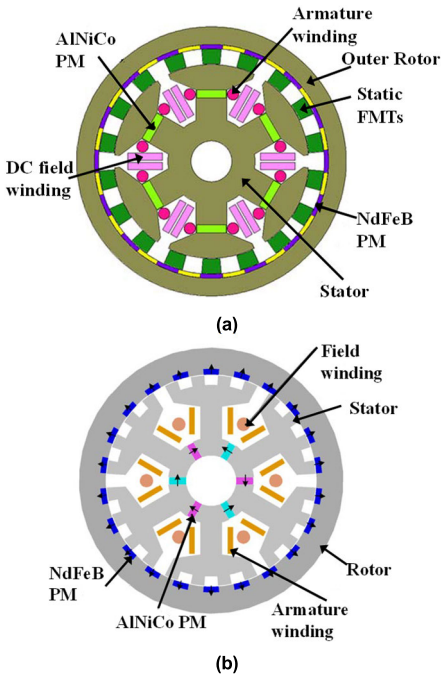

FIGURE 9. HEPM-V machines incorporating "memory machine" concept. (a) AlNiCo PMs in stator teeth [58]. (b) AlNiCo PMs in stator yoke [59].

it needs more space to accommodate the FMT. In other words, for the same split ratio (for inner rotor topology), the winding space for a split teeth stator will be smaller than its open slot counterpart. Moreover, the FMT short circuit some of the useful PM fluxes and thereby reduces the torque capability. A direct comparison between two outer rotor PM-V machines (∼30kW, 1000 rpm), one with open stator slot overlapping winding and the other with split teeth FSCW, is presented in [45]. The rotor structure is the same between these two machines with a V-shaped interior PM configuration. It is observed that the PM-V machine with an open slot and overlapping winding showed superior performance in terms of torque density, torque ripple, efficiency, etc. In addition, it is also revealed that the split teeth FSCW topology has serious magnetic saturation issues.

For conventional split teeth stator topology, the FMT is circumferentially and uniformly distributed. However, a novel design with an unequal pitch between adjacent FMT [see FIGURE 7(a)] is found to be able to improve the torque density by 20% [46]. Unequal pitch introduces extra working harmonics that help to increase the net torque. Similarly, to improve the fault-tolerant capability of the PM-V machines for safety-critical applications, single layer split teeth stator topology as shown in FIGURE 7(b) is investigated in [47]–[50]. The fault-tolerant stator tooth as highlighted in FIGURE 7(b) is made thinner to give more space for the windings. Split teeth stator topology with overlapping windings can also be found in the literature [51], [52]. This is to improve the torque density.

In summary, the 2-slot coil pitch is found to be a good tradeoff between the FSCW and overlapping winding with $q \geq 1$. The comparison between the FSCW and overlapping windings ($q \geq 1$) for direct-drive applications revealed that the latter has better torque capability. However, the FSCW would be a better choice for applications requiring high reliability, fault tolerance, and reduced volume with short end-windings [49].

C. HYBRID EXCITED PM-V (HEPM-V) MACHINES

Hybrid excited PM Vernier (HEPM-V) machines have an extra field winding in addition to the armature winding. By having a separate field excitation, the flux enhancement and flux weakening operations can be done in a more controlled way which is a drawback for most PM machines. Some of the possible arrangements of the field and armature windings along with the PMs are discussed below.

An HEPM-V machine with the field and armature windings sharing the same slot is presented in [53] as shown in FIGURE 8(a). Although the flux controllability is found to be better, the torque capability is compromised by having the extra field winding in the same stator slot. The field winding also contributes to extra copper loss, posing challenges for thermal management. This topology is further improved by having separate slots for the field windings. In this case, the field windings are either placed in the FMT slots [54], [55] as shown in FIGURE 8(b) or in a separate stator with a dual airgap structure [56]. However, the field windings have been used in continuous operation and thus generate a significant copper loss. To reduce the thermal risk of the rotor PMs for high-speed EV applications, the HEPM-V machine with all the excitations (including PMs) being located on the stator is investigated in [57].

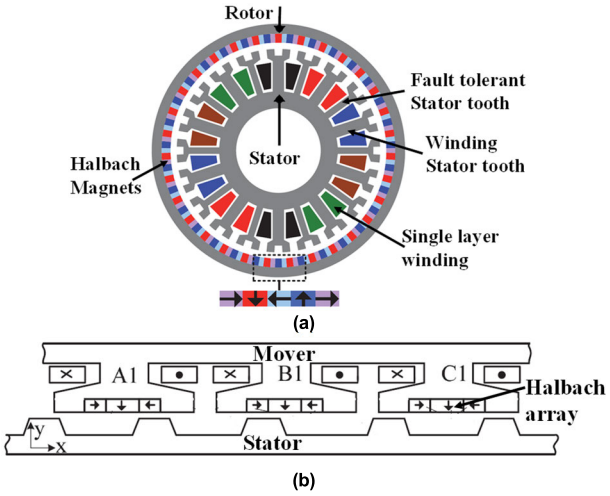

FIGURE 10. Single airgap PM-V machines with Halbach array PMs on the rotor. (a) Split teeth stator with Halbach array PMs on the rotor [47]. (b) Linear PM-V machine with Halbach array in the FMT slots of the mover with split teeth [61].

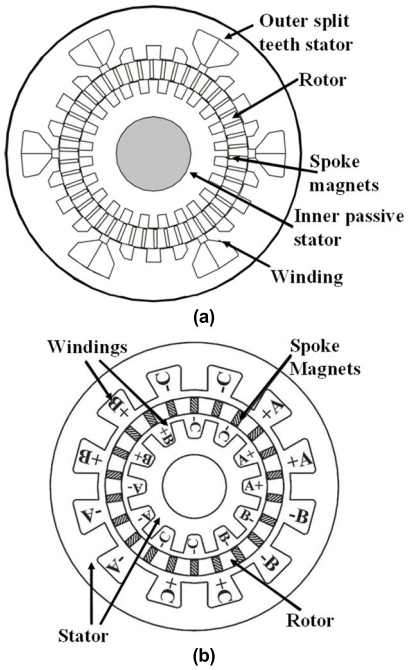

FIGURE 11. Dual stator PM-V machines with spoke array PM rotor sandwiched between the outer and inner stators. (a) With split teeth outer stator and a passive inner stator [65]. (b) With windings on both the inner and outer open slot stators [66].

To reduce the copper loss in the HEPM-V machines, ''memory machines'' as shown in FIGURE 9 with a combination of low coercive force PMs and NdFeB PMs are investigated [58]–[60]. In most cases, AlNiCo magnets are embedded in the stator, either in the teeth [58] or yoke [59], and their magnetization is altered by the DC field winding. The DC field winding is supplied only in the high-speed region where flux weakening is required and thus the copper loss can be significantly reduced.

In summary, the HEPM-V machines are the preferred topology for wide speed range applications requiring flux control, especially in the flux weakening region. However, the excess copper loss and associated thermal issues are the main challenges [55].

For the offshore wind power application with multi-MW power ratings, the electrical loading is expected to be high. Hence a form wound coil is desirable and therefore an open stator slot design would be a better choice amongst the stator structures discussed above. Although the split teeth stator is an attractive choice for a simple winding with reduced end winding length, the fast magnetic saturation would affect the performance at high electrical loadings. With high electrical loading, the power factor of PM-V machines can be even worse. Hence it would be better to design the PM-V machines with lower gear ratio to achieve reasonable power factor. This points towards an open slot stator design having an overlapping winding with $q \leq 1$.

IV. MAGNET ARRANGEMENTS ON ROTOR/STATOR

The structures of the PM-V machines are overall quite similar to the conventional PM machines and hence similar variants of rotor topologies can be found in the literature for PM-V machines. These can be mainly classified as shown in FIGURE 3.

A. HALBACH-ARRAY PM-V (HAPM-V) MACHINES

The PM-V machine with conventional SPM rotor is compared with two types of HAPM-V machines, one with ferromagnetic rotor yoke [see FIGURE 10(a)] and the other with nonmagnetic rotor yoke [47]. The comparison showed that the HAPM-V machine with ferromagnetic yoke has almost 20% higher torque density, 2% higher efficiency and better power factor compared to that with an SPM rotor. Whereas the design with a nonmagnetic yoke showed a comparable torque performance to that with an SPM rotor.

Similarly, a linear PM-V machine with Halbach array PMs installed in the FMT slots of the split teeth mover is investigated in [61] and [62], as shown in FIGURE 10(a). The proposed design is compared with a conventional flux reversal PM (FRPM) machine because of their similar structure. The proposed design can achieve 114% higher torque density with 32% lower PM usage [51]. To further improve the torque density and power factor, dual rotor/stator topologies are also presented in [63] and [64]. Halbach array topology in general helps to reduce the inter pole PM leakage flux which is critical in improving the power factor of the PM-V machines. However, compared to the conventional SPM-V machines, the PM assembly is more complicated and hence increases the manufacturing cost.

B. SPOKE-ARRAY PM-V (SAPM-V) MACHINES

There are several SAPM-V topologies reported in the literature due to their flux concentration feature. In most cases, to better utilize the PM, dual airgap topologies are adopted. A dual stator topology with a spoke array PM rotor

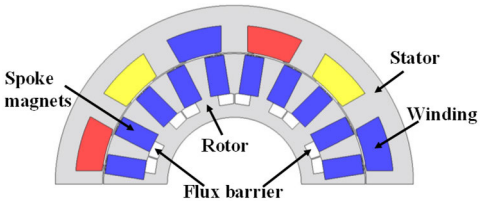

FIGURE 12. Single airgap SAPM-V machine topology with flux barriers in the rotor [72], [73].

sandwiched between an outer split teeth stator and an inner open slot stator is shown in FIGURE 11(a) [65]. The inner and outer stators are phase-shifted by one slot pitch enabling an easier path for the PM flux to link both the inner and outer stators. The proposed machine could achieve an efficiency of 90% with a power factor >0.75 at 150Nm torque and 130rpm rotor speed. Similarly, a dual stator PM-V machine with windings on both the inner and outer open slot stators as shown in FIGURE 11(b) is presented in [66]–[68]. The proposed design is then compared with a HAPM-V machine having a similar dual stator with a sandwiched SPM rotor (with ferromagnetic rotor back iron) and a single airgap [64]. The torque density of the proposed machine is found to be almost doubled compared to the other two topologies. In addition, the proposed machine could achieve a power factor of 0.91 compared to 0.73 (Halbach) and 0.85 (SPM rotor) of the other two machines.

Because of the flux concentration feature of the spoke magnets, the possibility of using ferrite magnets is also investigated for the proposed dual stator topology [see FIGURE 11(b)] [69]. The proposed design having ferrite PMs showed 33% higher torque production, higher efficiency

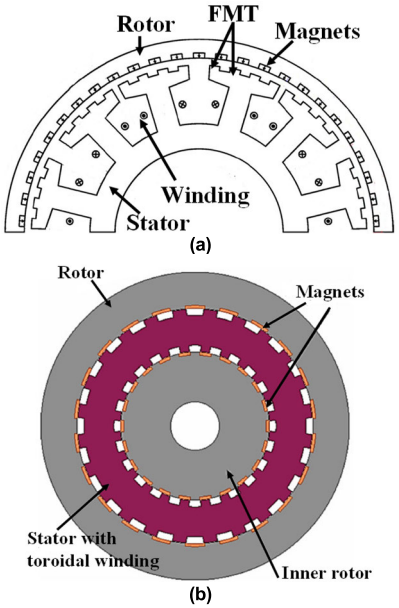

FIGURE 13. CPPM-V topologies with single and dual airgaps. (a) Single airgap with split teeth stator and FSCW [79]. (b) Dual consequent pole rotor with toroidal winding stator [80].

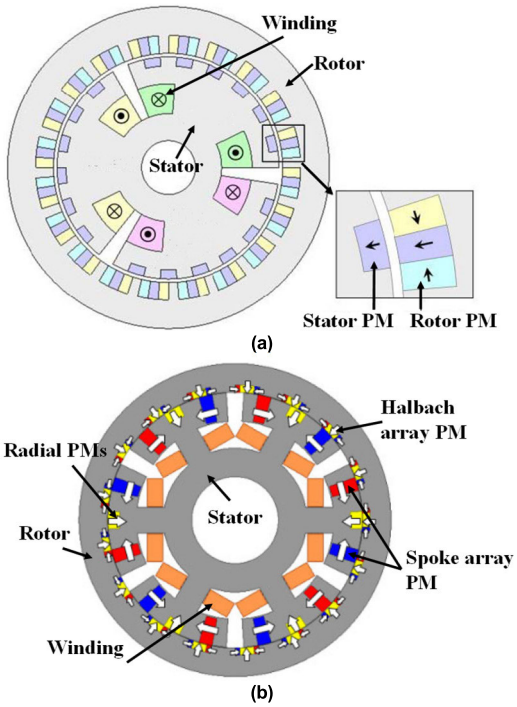

FIGURE 14. Single airgap MBPM-V machines with split teeth stator topology and PMs installed in the stator FMT slots. (a) Consequent pole Halbach and radial PMs [81]. (b) Halbach, spoke array and radial PMs [85].

but relatively lower power factor (0.72 *vs* 0.8) in comparison with a commercially available interior PM machine having rare-earth PMs [70].

The proposed design is further modified to mitigate the thermal issues faced by the inner stator windings [71]. The inner stator windings are removed and the stator core is used for directing the flux similar to that shown in FIGURE 11(a). As a result, the power factor is dropped to 0.78. To simplify the dual airgap structure, the proposed machine is further modified with a single airgap as shown in FIGURE 12 [72], [73]. To reduce the leakage from spoke array ferrite PMs, flux barriers are introduced at the bottom of the PMs. An extended back iron is provided for the armature flux without having to pass through the PMs. The torque density is found to be 59% higher compared to the conventional SPM-V machine. However, because of an easier flux path for the armature reaction, the power factor dropped to 0.62. Similarly, a single airgap outer rotor SAPM-V machine with an open stator slot and 2-slot coil pitch windings is investigated in [74]. The proposed machine could achieve a 30% higher torque density and a better power factor (0.92 *vs* 0.78) compared to a split teeth FSCW Vernier machine with an SPM outer rotor.

In summary, SAPM-V machines generally show better torque capability than their SPM-V counterparts because of their flux concentration feature. However, the single airgap topologies result in high PM leakage and therefore, in most cases, topologies with dual airgap are preferred. Hence spoke array PMs may not be the right choice for large

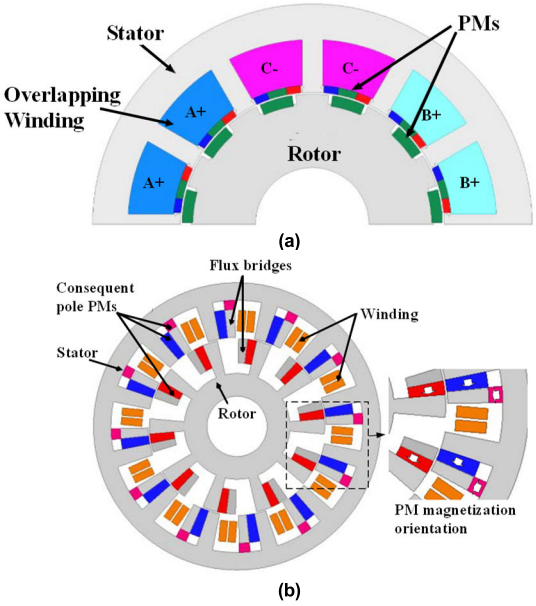

FIGURE 15. MBPM-V machines with open slot topologies. (a) Halbach array PMs in stator slot opening and consequent pole rotor [84]. (b) Consequent pole PMs on both the stator and rotor using flux bridges [85].

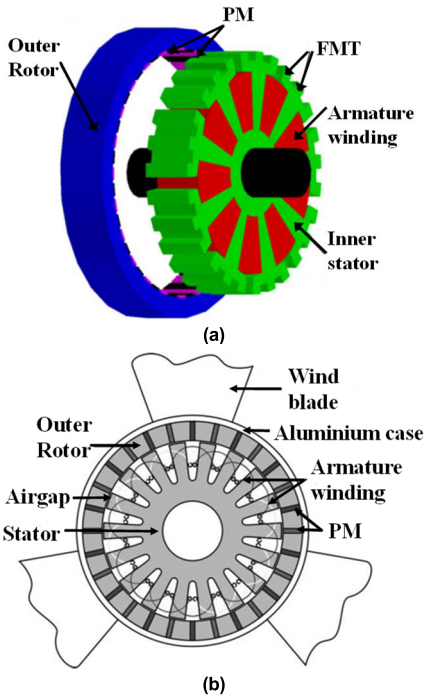

FIGURE 16. Vernier generators designed with split teeth and open slot stator for wind power application. (a) 2.2kW split teeth stator Vernier generator (150rpm) [95]. (b) 5kW open slot stator Vernier generator (214rpm) with 2-slot coil pitch [96].

size direct-drive offshore wind generators as the dual airgap would make the structure more complex.

C. CONSEQUENT POLE PM-V (CPPM-V) MACHINES

Consequent pole topologies (All the magnets have the same polarity and the return path of the PM flux is through the laminated steel core) have been extensively proposed for conventional and different flux-modulating PM machines [75], [75]–[79]. Generally, these topologies are proven to achieve higher torque to PM volume ratios compared to their conventional SPM counterparts.

Some of the consequent pole PM Vernier (CPPM-V) machines reported in literature are shown in FIGURE 13. Consequent pole topology has been used with both split teeth stator with FSCW [79] and open slot stator with toroidal winding [80] as shown in FIGURE 13(a) and (b), respectively. In most cases, the consequent pole concept is adopted in the Vernier machines that have the PMs installed on both the stator and rotor. These topologies will be discussed in detail in the next section.

D. MAGNETS ON BOTH SIDES OF THE PM-V (MBPM-V) MACHINES

Magnets on both sides of the PM Vernier (MBPM-V) topologies have PMs installed on both the rotor and stator. Most of the MBPM-V machines have a split teeth stator to utilize the FMT slots for installing the PMs [81]–[87]. This topology requires saliency in the rotor to modulate the stator PM flux and induce EMF in the stator windings. Hence, the rotors of the MBPM-V machines are generally consequent pole ones. Some of the MBPM-V machines with split teeth stator and FSCW are shown in FIGURE 14.

PM types such as radial, Halbach array, spoke array, etc. have been tried in different combinations to achieve better performances. The MBPM-V machines, in general, could achieve much higher torque density (2 to 3 times) and power factor than their conventional FSCW PM and split teeth stator PM-V machines [81], [82]. However, due to the presence of PMs on both the rotor and stator, the torque ripple for these topologies is found to be high [81]. Some of the torque ripple reduction techniques such as the introduction of flux barrier beneath the stator magnets [82], changing the angular pitch of the FMT slots [83], etc. have been investigated and found to be effective without compromising too much the torque capability.

MBPM-V machines with open stator slot topology are also investigated in [31], [88]–[94] as shown in FIGURE 15. The main challenge is the space constraint to installing PMs on the stator as there are no available separate slots like the FMT slots. Hence, the PMs have to be installed in the stator slots in close proximity to the windings. This can pose serious thermal challenges to the PMs leading to a high risk of potential irreversible demagnetization. High temperatures can also degrade the PM glue affecting its physical integrity. Otherwise, these topologies showed superior performance in terms of torque, power factor and efficiency.

Halbach array and consequent pole PM arrangements (including MBPM-V) show potential to reduce the PM volume and reduce leakage flux in PM-V machines. Hence they may be used for direct-drive offshore wind generators to

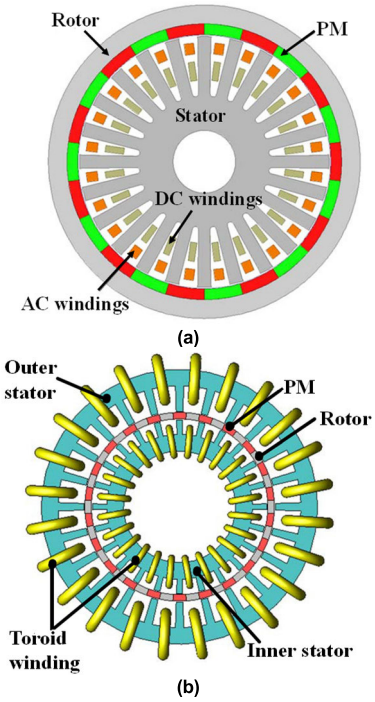

FIGURE 17. Vernier generator topologies for hybrid generation systems. (a) 433W double winding Vernier generator (272rpm) [97]. (b) Double stator toroidal winding Vernier generator (160mm outer diameter) [100].

further improve the torque density and power factor compared to the existing SPM-V machines.

E. PM-V MACHINES FOR WIND POWER APPLICATION

In most cases, the Vernier machines have been developed for direct-drive applications like wind power, tidal/wave power, electric propulsion, in-wheel traction, etc. In this section, we will highlight those Vernier generator topologies/designs which have been specifically reported in the literature for wind power applications.

Direct-drive wind generators, because of their low rotor speed, are generally designed with a large number of rotor poles to achieve an output frequency near the grid frequency. Therefore, in most cases, an outer rotor topology that can accommodate multiple poles is preferred. Moreover, the rotor with a large number of poles requires a thin back iron. This further helps to increase the airgap radius and thereby torque for an outer rotor topology. An outer rotor configuration also makes it possible to directly couple the generator rotor to the rotating turbine hub and thereby simplifies the drivetrain system. Because of these benefits, the Vernier generators proposed for wind power applications in the literature mostly has an outer rotor topology [17]–[19], [95]–[99].

The direct-drive wind generators have a ring-shaped structure because of their large diameter and thin back irons. To utilize the large space in the centre, topologies with an additional stator or rotor can be incorporated. However, more than one airgap increases the structural complexity, especially for large multi-MW wind generators. To mitigate this issue, an outer rotor topology with split teeth stator as shown in FIGURE 16(a) is proposed for a 2.2kW direct-drive Vernier generator [95]. The proposed topology is compared with two open slot Vernier generators with single (inner rotor) and double stator configurations. The authors claimed to achieve a better power density with less usage of raw materials compared to the other existing Vernier topologies. However, the comparison was performed for a small power rating with an outer diameter of 233mm. For high power ratings, with increasing electrical loading, the saturation issue of the split teeth stator topology is going to become more prominent. Hence, the conclusion may not be valid for high power ratings. Moreover, for large diameters, replacing the vacant space with active materials will result in a significantly heavy and expensive generator, which is not desirable.

The design, analysis and experimental verification of a 5kW Vernier generator with an open slot stator and 2-slot coil pitch windings as shown in FIGURE 16(b) is presented in [96]. The proposed design could achieve a high torque density of 31.1kNm/m^3 when compared to a radial field PM machine (10kNm/m^3) operating under a similar natural cooling condition. However, there is no mention of their achieved power factor which is critical for estimating the rating and cost of the power converter.

More design variants have been investigated specifically for hybrid generation systems [97], [100]. An outer rotor Vernier generator (433W, 100mm diameter) with separate DC and AC windings installed in the same stator slot as shown in FIGURE 17(a) is proposed to power an AC/DC

TABLE 2. Example of slot/pole number combinations for PM-V machines with $G_r = 5$ for a multi-MW direct-drive machine [20].

Machine Type	Stator slot number (N_s)	Rotor pole pair (P_r)	Stator winding pole pair (P_s)	Frequency	Stator coil inductance	Product (frequency× coil inductance)
conventional	480	80	80	F	L	FL
Vernier	48	40	8	0.5F	10L	5FL
Vernier	60	50	10	0.625F	8L	5FL
Vernier	72	60	12	0.75F	6.66L	5FL
Vernier	96	80	16	F	5L	5FL
Vernier	120	100	20	1.25F	4L	5FL
Vernier	192	160	32	2F	2.5L	5FL
Vernier	240	200	40	2.5F	2L	5FL
Vernier	360	300	60	3.75F	1.33L	5FL
Vernier	480	400	80	5F	L	5FL

microgrid [97]. A 6-phase winding is employed for the DC windings for generating a square wave voltage which is then rectified using a diode bridge rectifier. The slot/pole number combinations are carefully selected to improve the torque capability generated by both the DC and the 3-phase AC windings. However, the authors did not present any experimental results as a proof of concept. Similarly, a double stator topology with toroidal windings as shown in FIGURE 17(b) has been developed with a multi-mode operation feature for wind-photovoltaic generation systems [100]. The output voltage is modulated by appropriately connecting the terminals of each of the toroidal windings. A double stator can accommodate more toroidal windings and thereby more operating modes can be generated. The proposed topology could generate 54 different output voltages at rated speed by using different winding configurations. In addition, it could also generate the rated voltage for 3 different operating speeds. With this multi-mode operation feature along with the photovoltaic power, the authors have proposed a more flexible, reliable and efficient power generation system.

A novel design methodology for a 5kW direct-drive Vernier generator with split teeth and FSCW is presented in [98]. Wherein the author calculated the geometric parameters of the Vernier generator by estimating the generator circuit parameters for the maximum torque per ampere control scheme. A 15kW Vernier generator has been compared with a conventional SPM generator with FSCW [17], [18]. Both split teeth and open slot stator topologies have been investigated for Vernier generators. Finally, the open slot Vernier topology is chosen for the final comparison because of their higher power factor and lower torque ripple. The comparison showed that the Vernier generators have higher torque capability with less PM usage. They also showed better torque quality without using any torque ripple reduction techniques. However, since the conventional SPM machines often have higher power factors, their power converter has lower cost and smaller size. The overall cost of the SPM-V generator is comparable to that of its conventional counterpart at 15kW power level. The authors also built and tested the 15kW SPM-V machine. This is the largest prototype, in terms of size and power, built for PM-V machines in the literature.

V. CHALLENGES AND BENEFITS OF PM-V MACHINES FOR DIRECT-DRIVE OFFSHORE WIND POWER APPLICATIONS

The literature review revealed that a vast majority of research works about PM-V machines have been focused on small power ratings in the range of a few kWs. Recently, a few research works investigating the feasibility of PM-V machines for multi-MW direct-drive wind power applications have been published [19]–[24]. This section is dedicated to summarizing the challenges and benefits unfolded in these papers while scaling the PM-V machines from few kWs up to multi-MW power levels. Hence, the outcomes of these research works will be a good reference for any future work related to Vernier machines for high-power direct-drive applications.

It is worth noting that in most cases, a conventional SPM-V machine topology has been considered for the scaling study. As discussed before, the performance of PM-V machines is greatly influenced by the selection of G_r and the slot/pole number combinations. As an example, the comparison of slot/pole number combinations between the SPM-V and the conventional SPM machines for a 3MW direct-drive machine with $G_r = 5$ is shown in TABLE 2 [20]. The stator winding inductance and the operating frequency of the SPM-V machines (normalized to the frequency - F and and inductance - L of the conventional machines) are also highlighted. Understanding the variation of inductance and the operating frequency gives insights into different characteristics of the SPM-V machines with different slot/pole number combinations. The influence of G_r and the slot/pole number combinations on the performance of the SPM-V machines when the power rating is scaled up to multi-MW levels are discussed below:

A. TORQUE AND TORQUE RIPPLE

It is observed that the SPM-V machines exhibit higher torque capability towards lower slot/pole number combinations. This is because of reduced inter-pole PM and stator slot leakage fluxes as discussed before. These leakage fluxes are essentially a function of the ratio of rotor or stator pole pitch to magnetic airgap length (includes PM thickness and mechanical clearance). Hence, to represent the slot/pole numbers in a generic way across all power ratings, a new term called normalized pole pitch ($\bar{\tau_r}$) is introduced, defined as the ratio of rotor pole pitch to magnetic airgap length [21]. The trend of normalized average torque (using the torque generated by the corresponding conventional SPM machine as reference) with $\bar{\tau_r}$ for different power ratings, such as 3kW, 0.5MW, 3MW, 5MW and 10MW, was studied in [21] and [22]. It was an interesting observation that the normalized torque curves of these power ratings overlapped each other as a function of $\bar{\tau_r}$. This indicated that the torque performance of the SPM-V machines compared to the conventional SPM machines is largely defined by the design choice of $\bar{\tau_r}$. It is observed that the SPM-V machines could achieve a higher torque density than the conventional SPM machine when designed with a $\bar{\tau_r} > 2.2$. The value of $\bar{\tau_r}$ to achieve the optimal torque of SPM-V machine is limited by the magnetic saturation. As can be observed from TABLE 2, the inductance of the winding increases towards lower slot/pole number combinations or higher $\bar{\tau_r}$. As the electrical loading of the machine increases towards multi-MW power ratings, the effect of saturation increases and the optimal $\bar{\tau_r}$ value decreases. In any case, it was observed that the SPM-V machines, even at multi-MW power ratings, can achieve a higher torque density (60% to 80% higher) compared to the conventional SPM machines. This would mean that the SPM-V machines can be designed with a much lower volume than the conventional SPM machines for the same power level. A lower volume

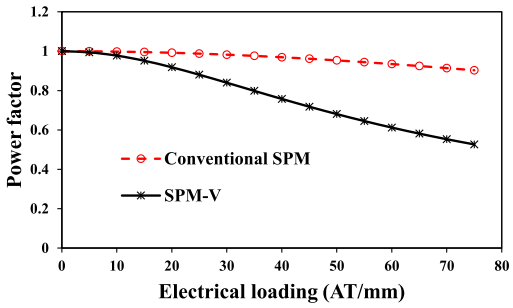

FIGURE 18. Comparison of variation of power factor with electrical loading between the conventional SPM and SPM-V machines [23].

would also mean a smaller footprint, more free space inside the nacelle making the maintenance easier and also may reduce the existing logistic challenges with large direct-drive machines. This is one of the most significant benefits of Vernier machines. It is worth noting that a reduced volume may not lead to a machine with reduced mass or cost and this is further discussed in detail in section V. C.

The assessment of the torque ripple is very critical for low-speed high torque direct-drive applications. Similar to low power ratings, the torque ripple of the SPM-V machines was found to be inherently lower than the conventional SPM machines even at multi-MW power levels [20], [24]. The comparison was made without incorporating any torque ripple reduction techniques like PM shaping, skewing, etc. SPM-V machines even without using these techniques can achieve torque ripple below the required limits and hence can make the manufacturing process simpler and less costly.

B. POWER FACTOR

Several studies, mostly conducted in smaller machines, have shown that the PM-V machines have a relatively lower power factor (∼0.6-0.8) compared to conventional PM machines. The poor power factor of the PM-V machines is due to their high synchronous reactance. As shown in TABLE 2, irrespective of the chosen slot/pole number combinations, the product of inductance and operating frequency for the PM-V machines is almost G_r times that of the conventional PM machines. Moreover, the consideration of inter-pole PM and the stator slot leakage fluxes will vary the magnitude of induced EMF and the stator winding inductance across different slot/pole number combinations. Accordingly, the power factor achieved across slot/pole number combinations will vary. Hence, the power factor is better towards lower slot/pole number combinations or high $\bar{\tau_r}$, due to reduced leakage fluxes [20], [23]. In addition to these leakage fluxes, it was also revealed that there is a significant amount of PM flux that actually enters the stator core back iron and still does not contribute to the induced EMF due to the large coil pitch to rotor pole ratio [21]. This leakage flux is found to be much more dominant than other leakage fluxes discussed above. This is the reason why the PM-V machines designed with low slot/pole numbers or high $\bar{\tau_r}$ still have low power factors even after having negligible inter-pole PM and stator slot leakage fluxes.

With increasing G_r, the coil pitch to rotor pole pitch ratio increases and therefore the power factor reduces further. The study conducted at 1MW and 3MW power levels for the Vernier machines with different gear ratios, i.e., $G_r \geq 5$ (distributed overlapping windings) and $G_r < 5$ (2-slot pitch distributed winding), have proposed $G_r \leq 5$ as the best choice to achieve a relatively good power factor and reduced active mass [19]. This is different from the trend observed in small power machines where lower G_r may not be the best choice.

An analytical model, considering all the leakage fluxes has been presented in [23] for the SPM-V machines. Through the analytical modeling and FEA simulation, it was revealed that, unlike the conventional SPM machines, the power factor of the SPM-V machines significantly drops with increasing electrical loading. The variations of power factor with electrical loading between the conventional SPM and SPM-V machines calculated using the analytical model are shown in FIGURE 18. Even with a relatively small $G_r = 5$, the power factors of the multi-MW SPM-V machines (with electrical loading in the range 50-60 AT/mm) are in the range of ∼0.4-0.5, which is already very low [23]. The conventional SPM machines could still achieve a relatively good power factor of about 0.8-0.9 at these MW power levels. This is one of the significant challenges that unfolded during the scaling study for the SPM-V machines. This is going to negatively impact the power converter rating and their losses, affecting the overall system-level efficiency of the drivetrain.

C. MASS AND COST

With the increasing size of the direct-drive generator for high power offshore wind applications, it is critical to reduce their mass and cost. Because of their relatively small speed (10-25rpm), the conventional direct-drive generators are designed with a high number of poles to achieve a frequency matching with that of the grid. The high pole number results in a design with a thinner rotor and stator back irons. Hence, the direct-drive generators have a ring-shaped structure with a large diameter and relatively small axial length. Large and massive structural components are required to support the active materials (that generate the power) against the high stresses acting on the stator and rotor. At around 5MW power level, the structural mass is found to contribute to 80% of the total generator mass. Whereas the structural and active materials almost equally contribute to the total generator cost [22]. Hence, it is important to consider both the active and structural materials of the generator while comparing different generator topologies. Amongst the active materials, lamination mass is the most dominant one, contributing to almost 60% of the total active mass at multi-MW power level [19].

To achieve higher torque than the conventional SPM machines, the PM-V machines are generally designed with lower slot/pole number combinations or higher $\bar{\tau_r}$. This increases their winding inductance and the flux per pole

resulting in large stator and rotor back iron thicknesses to limit the magnetic saturation. However, for the same power level, the PM-V machines can be designed with a smaller diameter or volume because of their higher torque density capability. This in turn can help to reduce the overall active and structural material masses and costs. The overall mass of an SPM-V generator at around 500kW is found to be 26% lower than that of the conventional SPM generator. This includes a 45% reduction in the active mass and a 13% reduction in structural mass [22]. However, the benefit in the active mass reduction is diminishing when the power is scaled up to multi-MW levels. This is because, with increasing power rating or electrical loading, the conventional SPM generators are designed with much larger stator slots to increase the heat dissipation area and thereby improve the thermal performance. Hence, the conventional SPM machines have thinner back irons for the stator and rotor resulting in lower active mass. However, the SPM-V machines still need to be designed in the same range of $\bar{\tau}_r$ to achieve a higher torque capability than their conventional counterparts. At around 10MW power level, the active mass of the SPM-V generator is found to be 3-4% higher than the conventional SPM machine. But a 10% reduction in the structural mass has given the edge to the SPM-V machine with a 7% overall mass reduction [22].

From the cost perspective, at 500kW, the SPM-V machine is 25% less costly than the conventional SPM machines. This includes a 32% and 13% cost saving from active and structural materials, respectively. The airgap length of the PM machine is generally designed as 0.1% of its airgap diameter [101]. Because of the reduced diameter of the SPM-V generator and thereby the airgap length, they utilize less magnet volume for the same output power. Since the cost of the active material is mainly driven by the magnets, the SPM-V machine could reduce the cost by 10% even at 10MW power level. Furthermore, a 10% reduction in the structural material resulted in a 10% reduction in the overall generator cost. However, because of the poor power factor ($\sim$0.4-0.5) of the SPM-V generators, the power converter cost has significantly increased by almost 50% across power ratings ranging from 500kW to 10MW. This has increased the overall system-level cost of the SPM-V generator by 6-12%. A similar conclusion has been drawn in [19] proposing $G_r \leq 5$ as the best choice for PM-V machine to achive the minimum mass and cost at mutli-MW power level.

Although the SPM-V machines show a potential to reduce the overall mass and cost of the direct-drive generator, there are a few more design aspects to be considered which can pose more challenges to the existing benefits. The system-level comparisons between the conventional SPM and the SPM-V generators presented in [22] are performed for the same copper loss between these two types of machines. However, to achieve high torque density, the SPM-V machines are generally designed for high $\bar{\tau}_r$ (>2.2) which results in much smaller stator slots than the conventional SPM machines at multi-MW power levels [24]. This in turn makes the copper loss per stator slot surface area much higher than the conventional SPM generators and therefore better cooling technologies might be needed. To make the copper loss per stator slot surface area the same between these two types of machines, the SPM-V machine needs either larger slot depths or reduced electrical loading. The former would indirectly increase the active mass and cost of the SPM-V generators and the latter could reduce their torque capability. Based on the comparison carried out in [22], it is found that the copper loss per stator slot surface area is almost 2 to 3 times higher than that of the conventional SPM machines at multi-MW power levels. This can negatively impact the benefits of the SPM-V generators in terms of cost saving and mass reduction.

D. EFFICIENCY

For direct-drive wind power applications, the PM-V machines showed a comparable efficiency with that of the conventional PM machines [17], [22], [102]. It is worth noting that the analyses performed in these studies are based on machines using a laminated rotor and segmented magnets. This arrangement is mainly due to the fact that the fundamental armature MMF in a PM-V machine is asynchronous with the rotor mechanical speed. As a result, if solid rotor iron core and unsegmented magnets are used, significant eddy current loss will be generated in them. However, the laminated rotor with segmented magnets will increase the cost and manufacturing complexity of the PM-V machines, particularly for the large ones used in offshore wind power applications. Moreover, a solid rotor frame may be required to stack the laminations which will compromise the torque for the same machine outer diameter.

Due to the low power factor of the PM-V machines, their associated generator side power converter losses increase significantly. For the same terminal voltage as the conventional PM generator, the converter currents will be much higher and accordingly its losses increase. This reduces the overall system-level efficiency by 2-3% at mutli-MW power levels [22]. Since the power factor of the PM-V machines is largely driven by the electrical loading of the machine at multi-MW power levels, the scope for further improvement is small [23]. So if comparing for the same grid power between these two types of machines, the SPM-V machine will have to be designed for larger generator power to offset the excess converter losses.

E. IRREVERSIBLE DEMAGNETIZATION

Unlike the conventional PM machines, the PM-V machines have a larger number of rotor poles within one coil pitch depending on G_r the machine is designed for. For example, a PM-V machine with $G_r = 5$ will have 5 rotor poles within one stator coil pitch. Therefore, the magnet thickness in a PM-V machine is much smaller than that of a conventional SPM machine for the same magnet volume. Moreover, the PM-V machine has to be designed with $\bar{\tau}_r > 2.2$ to achieve higher torque capability. This results in an increased winding inductance than the conventional PM machine and thereby

the magnets are exposed to a higher armature reaction. This poses a higher risk of potential irreversible demagnetization [20]. Therefore, the PM-V machines might need to be designed with thicker magnets or with reduced electrical loading, leading to increased overall machine cost or reduced torque capability.

VI. CONCLUSION

The literature review, mostly focused on small power machines, has shown that the PM-V machines have the potential to improve the torque density of direct-drive machines without compromising too much on the power factor (∼0.6-0.9). The scaling study performed over a wide range of power ratings (from few kWs to multi-MWs) has proven that the PM-V machines can still achieve a torque density 60-80% higher than that of the conventional SPM machines. However, the power factor has shown a significant drop to around 0.4-0.5 due to significantly increased electric loading in combination with the increased PM flux leakage. This has resulted in an increased cost and reduced efficiency for the whole drivetrain system (generator + power converter).

One of the main benefits that a PM-V machine offers is the significant reduction in machine volume for the same output power. However, to achieve a high torque density and to have a similar thermal performance as a conventional SPM machine, the PM-V machine uses much more iron core material. This increases the mass and cost of the machine. Hence, the PM-V machines may not help to improve the power to weight or power to cost ratio in comparison with the existing conventional PM machines at multi-MW power levels. Moreover, the poor power factor significantly increases power converter losses, resulting in a 2-3% reduction in the overall system-level efficiency. Therefore, unlike the trend shown in small power machines, the Vernier machines are facing much more challenges at multi-MW power levels making them less attractive for current direct-drive offshore wind power applications. However, in the future when the power rating increases to >20MW, the reduced volume of the PM-V machines may offer significant savings for the structural mass and cost, making them more competitive against their conventional counterparts.

REFERENCES

[1] L. Joyce and F. Zhao. (Aug. 2020). *Global Offshore Wind Report 2020*. Global Wind Energy Council (GWEC). [Online]. Available: https://gwec.net/global-offshore-wind-report-2020/

[2] E. Simon, H. Maureen, S. Joachim, and P. Bentham. (Sep. 2019). *Analysis: Record-Low Price for U.K. Offshore Wind Cheaper Than Existing Gas Plants by 2023*. [Online]. Available: https://www.carbonbrief.org/analysis-record-low-U.K.-offshore-wind-cheaper-than-existing-gas-plants-by-2023

[3] W. Ryan, S. Joachim, P. Bentham, and H. Maureen, "Sky's the limit? Reducing wind energy costs through increased turbine size," Berkeley Lab., Berkeley, CA, USA, Tech. Rep. LBNL-1005717, Dec. 2016.

[4] (Nov. 2019). *Offshore Wind Outlook 2019*. Paris, France. [Online]. Available: https://www.iea.org/reports/offshore-wind-outlook-2019

[5] J. Carroll, A. McDonald, and D. Mcmillan, "Failure rate, repair time and unscheduled O&M cost analysis of offshore wind turbines," *Wind Energy*, vol. 19, no. 6, pp. 1107–1119, Jun. 2016.

[6] A. Koltsidopoulos Papatzimos, T. Dawood, and P. Thies, "Data insights from an offshore wind turbine gearbox replacement," in *Proc. J. Phys., Conf.*, vol. 1104, 2018, Art. no. 012003.

[7] H. Polinder, F. F. A. van der Pijl, G.-J. de Vilder, and P. J. Tavner, "Comparison of direct-drive and geared generator concepts for wind turbines," *IEEE Trans. Energy Convers.*, vol. 21, no. 3, pp. 725–733, Sep. 2006.

[8] Z. Zhang, A. Chen, A. Matveev, R. Nilssen, and A. Nysveen, "High-power generators for offshore wind turbines," *Energy Proc.*, vol. 35, pp. 52–61, Jan. 2013.

[9] R. S. Semken, M. Polikarpova, P. Roytta, J. Alexandrova, J. Pyrhonen, J. Nerg, A. Mikkola, and J. Backman, "Direct-drive permanent magnet generators for high-power wind turbines: Benefits and limiting factors," *IET Renew. Power Generat.*, vol. 6, no. 1, pp. 1–8, Jan. 2012.

[10] T. M. Jahns, "The expanding role of PM machines in direct-drive applications," in *Proc. Int. Conf. Electr. Mach. Syst.*, Beijing, China, Aug. 2011, pp. 1–6.

[11] S. Alshibani, V. G. Agelidis, and R. Dutta, "Lifetime cost assessment of permanent magnet synchronous generators for MW level wind turbines," *IEEE Trans. Sustain. Energy*, vol. 5, no. 1, pp. 10–17, Jan. 2014.

[12] J. Carroll, A. McDonald, I. Dinwoodie, D. Mcmillan, M. Revie, and I. Lazakis, "Availability, operation and maintenance costs of offshore wind turbines with different drive train configurations," *Wind Energy*, vol. 20, no. 2, pp. 361–378, Feb. 2017.

[13] A. Tovar-Barranco, D. J. Gomez, A. Lopez-de-Heredia, and I. Villar, "High torque density transverse flux permanent magnet machine design for wind power generation," in *Proc. XXII Int. Conf. Electr. Mach. (ICEM)*, Sep. 2016, pp. 782–788.

[14] A. B. Kjaer, S. Korsgaard, S. S. Nielsen, L. Demsa, and P. O. Rasmussen, "Design, fabrication, test, and benchmark of a magnetically geared permanent magnet generator for wind power generation," *IEEE Trans. Energy Convers.*, vol. 35, no. 1, pp. 24–32, Mar. 2020.

[15] R. Zeinali and O. Keysan, "A rare-Earth free magnetically geared generator for direct-drive wind turbines," *Energies*, vol. 12, no. 3, p. 447, Jan. 2019.

[16] R. Qu, D. Li, and J. Wang, "Relationship between magnetic gears and Vernier machines," in *Proc. Int. Conf. Elect. Mach. Syst.*, Beijing, China, Aug. 2011, pp. 1–6.

[17] P. M. Tlali, R.-J. Wang, and S. Gerber, "Comparison of PM Vernier and conventional synchronous 15 kW wind generators," in *Proc. XIII Int. Conf. Electr. Mach. (ICEM)*, Alexandroupoli, Greece, Sep. 2018, pp. 2065–2071.

[18] P. M. Tlali, R.-J. Wang, S. Gerber, C. D. Botha, and M. J. Kamper, "Design and performance comparison of Vernier and conventional PM synchronous wind generators," *IEEE Trans. Ind. Appl.*, vol. 56, no. 3, pp. 2570–2579, May 2020.

[19] P. M. Tlali and R.-J. Wang, "PM Vernier machine for utility scale wind generator applications: Design and evaluation," in *Proc. Int. Conf. Electr. Mach. (ICEM)*, Gothenburg, Sweden, Aug. 2020, pp. 2637–2643.

[20] D. K. P. Kumar, G. J. Li, Z. Q. Zhu, M. P. Foster, D. A. Stone, A. Griffo, M. Odavic, R. Clark, and A. Thomas, "Influence of demagnetization on selecting the optimum slot/pole number combination for 3MW surface mounted permanent magnet Vernier machine," in *Proc. 22nd Int. Conf. Electr. Mach. Syst. (ICEMS)*, Harbin, China, Aug. 2019, pp. 1–6.

[21] D. K. Kana Padinharu, G. J. Li, Z. Q. Zhu, M. P. Foster, D. A. Stone, A. Griffo, R. Clark, and A. Thomas, "Scaling effect on electromagnetic performance of surface-mounted permanent-magnet Vernier machine," *IEEE Trans. Magn.*, vol. 56, no. 5, May 2020, Art. no. 8100715.

[22] D. K. K. Padinharu, G.-J. Li, Z.-Q. Zhu, R. Clark, A. S. Thomas, and Z. Azar, "System-level investigation of multi-MW direct-drive wind power PM Vernier generators," *IEEE Access*, vol. 8, pp. 191433–191446, 2020.

[23] D. K. Kana Padinharu, G. Li, Z. Zhu, R. Clark, Z. Azar, and A. Thomas, "Investigation of scaling effect on power factor of permanent magnet Vernier machines for wind power application," *IET Electr. Power Appl.*, vol. 14, no. 11, pp. 2136–2145, Nov. 2020.

[24] D. K. Kana Padinharu, G. J. Li, Z. Q. Zhu, Z. Azar, R. Clark, and A. Thomas, "Effect of airgap length on electromagnetic performance of surface mounted permanent magnet Vemier machine," in *Proc. Int. Conf. Elect. Mach. (ICEM)*, vol. 1, 2020, pp. 1882–1888.

[25] S. Hyoseok, N. Niguchi, and K. Hirata, "Characteristic analysis of surface permanent-magnet Vernier motor according to pole ratio and winding pole number," *IEEE Trans. Magn.*, vol. 53, no. 11, pp. 1–4, Nov. 2017.

[26] B. Kim and T. A. Lipo, "Operation and design principles of a PM Vernier motor," *IEEE Trans. Ind. Appl.*, vol. 50, no. 6, pp. 3656–3663, Nov. 2014.
[27] D. Li, R. Qu, and J. Li, "Topologies and analysis of flux-modulation machines," in *Proc. Energy Convers. Congr. Expo. (ECCE)*, Montreal, QC, Canada, Sep. 2015, pp. 2153–2160.
[28] A. Toba and T. A. Lipo, "Generic torque-maximizing design methodology of surface permanent-magnet Vernier machine," *IEEE Trans. Ind. Appl.*, vol. 36, no. 6, pp. 1539–1546, Nov. 2000.
[29] D. Li, R. Qu, J. Li, L. Xiao, L. Wu, and W. Xu, "Analysis of torque capability and quality in Vernier permanent-magnet machines," *IEEE Trans. Ind. Appl.*, vol. 52, no. 1, pp. 125–135, Jan. 2016.
[30] L. Wu, R. Qu, D. Li, and Y. Gao, "Influence of pole ratio and winding pole numbers on performance and optimal design parameters of surface permanent-magnet Vernier machines," *IEEE Trans. Ind. Appl.*, vol. 51, no. 5, pp. 3707–3715, Sep. 2015.
[31] A. Ishizaki, "Theory and optimum design of PM Vernier motor," in *Proc. IEEE Energy Convers. Congr. Expo. (ECCE)*, Sep. 1995, pp. 208–212.
[32] M. J. F. Llibre and M. D. Matt, "Harmonic study of the effort in the Vernier reluctance magnet machine," in *Proc. Int. Conf. Elect. Mach. (ICEM)*, Istanbul, Turkey, 1998, pp. 1664–1669.
[33] K. Xie, D. Li, R. Qu, X. Ren, M. R. Shah, and Y. Pan, "A new perspective on the PM Vernier machine mechanism," *IEEE Trans. Ind. Appl.*, vol. 55, no. 2, pp. 1420–1429, Mar. 2019.
[34] J. Li and K. T. Chau, "Performance and cost comparison of permanent-magnet Vernier machines," *IEEE Trans. Appl. Supercond.*, vol. 22, no. 3, Jun. 2012, Art. no. 5202304.
[35] L. Wu, R. Qu, and D. Li, "Analysis of eddy current losses in surface-mounted permanent magnet Vernier machines," in *Proc. IEEE Int. Electr. Mach. Drives Conf. (IEMDC)*, May 2017, pp. 1–6.
[36] D. Li, T. Zou, R. Qu, and D. Jiang, "Analysis of fractional-slot concentrated winding PM Vernier machines with regular open-slot stators," *IEEE Trans. Ind. Appl.*, vol. 54, no. 2, pp. 1320–1330, Mar./Apr. 2018.
[37] Z. Q. Zhu and Y. Liu, "Analysis of air-gap field modulation and magnetic gearing effect in fractional-slot concentrated-winding permanent-magnet synchronous machines," *IEEE Trans. Ind. Electron.*, vol. 65, no. 5, pp. 3688–3698, May 2018.
[38] Y. Liu and Z. Q. Zhu, "Influence of gear ratio on the performance of fractional slot concentrated winding permanent magnet machines," *IEEE Trans. Ind. Electron.*, vol. 66, no. 10, pp. 7593–7602, Oct. 2019.
[39] Y. Liu, H. Y. Li, and Z. Q. Zhu, "A high-power factor Vernier machine with coil pitch of two slot pitches," *IEEE Trans. Magn.*, vol. 54, no. 11, pp. 1–5, Nov. 2018.
[40] D. Li, R. Qu, J. Li, and W. Xu, "Consequent-pole toroidal-winding outer-rotor Vernier permanent-magnet machines," *IEEE Trans. Ind. Appl.*, vol. 51, no. 6, pp. 4470–4481, Nov. 2015.
[41] A. Toba and T. A. Lipo, "Novel dual-excitation permanent magnet Vernier machine," in *Proc. Conf. Rec. IEEE Ind. Appl. Conf. 34th IAS Annu. Meeting*, vol. 4, Oct. 1999, pp. 2539–2544.
[42] S. Niu, S. L. Ho, W. N. Fu, and L. L. Wang, "Quantitative comparison of novel Vernier permanent magnet machines," *IEEE Trans. Magn.*, vol. 46, no. 6, pp. 2032–2035, Jun. 2010.
[43] S. Shafiei, M. A. Noroozi, J. Milimonfared, and H. Lesani, "Performance comparison of outer rotor permanent magnet Vernier motor for direct drive systems," in *Proc. 11th Power Electron., Drive Syst., Technol. Conf. (PEDSTC)*, Feb. 2020, pp. 1–4.
[44] H. Li, Z. Q. Zhu, and Y. Liu, "Optimal number of flux modulation pole in Vernier permanent magnet synchronous machines," *IEEE Trans. Ind. Appl.*, vol. 55, no. 6, pp. 5747–5757, Nov. 2019.
[45] G. Xu, L. Jian, W. Gong, and W. Zhao, "Quantitative comparison of flux-modulated interior permanent magnet machines with distributed windings and concentrated windings," *Prog. Electromagn. Res.*, vol. 129, pp. 109–123, 2012.
[46] T. Zou, D. Li, R. Qu, D. Jiang, and J. Li, "Advanced high torque density PM Vernier machine with multiple working harmonics," *IEEE Trans. Ind. Appl.*, vol. 53, no. 6, pp. 5295–5304, Nov. 2017.
[47] L. Xu, G. Liu, W. Zhao, J. Ji, and X. Fan, "High-performance fault tolerant Halbach permanent magnet Vernier machines for safety-critical applications," *IEEE Trans. Magn.*, vol. 52, no. 7, pp. 1–4, Jul. 2016.
[48] G. Liu, J. Yang, W. Zhao, J. Ji, Q. Chen, and W. Gong, "Design and analysis of a new fault-tolerant permanent-magnet Vernier machine for electric vehicles," *IEEE Trans. Magn.*, vol. 48, no. 11, pp. 4176–4179, Nov. 2012.
[49] K. Du, W. Zhao, L. Xu, and J. Ji, "Design of a new fault-tolerant linear permanent-magnet Vernier machine," *IEEE J. Emerg. Sel. Topics Ind. Electron.*, vol. 1, no. 2, pp. 172–181, Oct. 2020.
[50] J. Yang, G. H. Liu, W. X. Zhao, Q. Chen, Y. C. Jiang, L. G. Sun, and X. Y. Zhu, "Quantitative comparison for fractional-slot concentrated-winding configurations of permanent-magnet Vernier machines," *IEEE Trans. Magn.*, vol. 49, no. 7, pp. 3826–3829, Jul. 2013.
[51] L. Xu, G. Liu, W. Zhao, J. Ji, H. Zhou, W. Zhao, and T. Jiang, "Quantitative comparison of integral and fractional slot permanent magnet Vernier motors," *IEEE Trans. Energy Convers.*, vol. 30, no. 4, pp. 1483–1495, Dec. 2015.
[52] S. Zhu, T. Cox, Z. Xu, and C. Gerada, "Analysis of a five-phase PM Vernier machine topology with two-slot pitch winding," in *Proc. IEEE Energy Convers. Congr. Expo. (ECCE)*, Detroit, MI, USA, Oct. 2020, pp. 1174–1179.
[53] C. Liu, J. Zhong, and K. T. Chau, "A novel flux-controllable Vernier permanent-magnet machine," *IEEE Trans. Magn.*, vol. 47, no. 10, pp. 4238–4241, Oct. 2011.
[54] H. Wang, S. Fang, H. Yang, H. Lin, D. Wang, Y. Li, and C. Jiu, "A novel consequent-pole hybrid excited Vernier machine," *IEEE Trans. Magn.*, vol. 53, no. 11, pp. 1–4, Nov. 2017.
[55] H. Wang, S. Fang, H. Yang, H. Lin, Y. Li, L. Qin, and Y. Zhou, "Loss calculation and temperature field analysis of consequent-pole hybrid excited Vernier machine," *IEEE Trans. Magn.*, vol. 53, no. 11, pp. 1–5, Nov. 2017.
[56] L. Wei and T. Nakamura, "A novel dual-stator hybrid excited permanent magnet Vernier machine with Halbach-array PMs," *IEEE Trans. Magn.*, vol. 57, no. 2, pp. 1–5, Feb. 2021.
[57] L. Xu, G. Liu, W. Zhao, and J. Ji, "Hybrid excited Vernier machines with all excitation sources on the stator for electric vehicles," *Prog. Electromagn. Res. M*, vol. 46, pp. 113–123, 2016.
[58] C. Liu, K. T. Chau, and C. Qiu, "Design and analysis of a new magnetic-geared memory machine," *IEEE Trans. Appl. Supercond.*, vol. 24, no. 3, pp. 1–5, Jun. 2014.
[59] H. Yang, H. Lin, Z. Q. Zhu, S. Fang, and Y. Huang, "Novel flux-regulatable dual-magnet Vernier memory machines for electric vehicle propulsion," *IEEE Trans. Appl. Supercond.*, vol. 24, no. 5, pp. 1–5, Oct. 2014.
[60] H. Yang, H. Lin, Z.-Q. Zhu, S. Fang, and Y. Huang, "A dual-consequent-pole Vernier memory machine," *Energies*, vol. 9, no. 3, p. 134, Feb. 2016.
[61] J. Ji, W. Zhao, Z. Fang, J. Zhao, and J. Zhu, "A novel linear permanent-magnet Vernier machine with improved force performance," *IEEE Trans. Magn.*, vol. 51, no. 8, pp. 1–10, Aug. 2015.
[62] S. Wang, W. Zhao, J. Ji, L. Xu, and J. Zheng, "Magnetic gear ratio effects on performances of linear primary permanent magnet Vernier motor," *IEEE Trans. Appl. Supercond.*, vol. 26, no. 7, pp. 1–5, Oct. 2016.
[63] A. Allahyari, A. Mahmoudi, and S. Kahourzade, "High power factor dual-rotor Halbach array permanent-magnet Vernier machine," in *Proc. IEEE Int. Conf. Power Electron., Drives Energy Syst. (PEDES)*, Dec. 2020, pp. 1–6.
[64] D. Li, R. Qu, and Z. Zhu, "Comparison of Halbach and dual-side Vernier permanent magnet machines," *IEEE Trans. Magn.*, vol. 50, no. 2, pp. 801–804, Feb. 2014.
[65] I. Boldea, L. Tutelea, and M. Topor, "Theoretical characterization of three phase flux reversal machine with rotor-PM flux concentration," in *Proc. 13th Int. Conf. Optim. Electr. Electron. Equip. (OPTIM)*, May 2012, pp. 472–476.
[66] D. Li, R. Qu, and T. Lipo, "High-power-factor Vernier permanent-magnet machines," *IEEE Trans. Ind. Appl.*, vol. 50, no. 6, pp. 3664–3674, Dec. 2014.
[67] D. Li, R. Qu, W. Xu, J. Li, and T. A. Lipo, "Design procedure of dual-stator spoke-array Vernier permanent-magnet machines," *IEEE Trans. Ind. Appl.*, vol. 51, no. 4, pp. 2972–2983, Jul. 2015.
[68] B. Kim and T. A. Lipo, "Analysis of a PM Vernier motor with spoke structure," *IEEE Trans. Ind. Appl.*, vol. 52, no. 1, pp. 217–225, Jan./Feb. 2016.
[69] Z. S. Du and T. A. Lipo, "An improved rotor design for dual-stator Vernier ferrite permanent magnet machines," in *Proc. IEEE Int. Electr. Mach. Drives Conf. (IEMDC)*, May 2017, pp. 1–8.
[70] Z. S. Du and T. A. Lipo, "Torque performance comparison between a ferrite magnet Vernier motor and an industrial interior permanent magnet machine," *IEEE Trans. Ind. Appl.*, vol. 53, no. 3, pp. 2088–2097, Feb. 2017.

[71] D. Li, R. Qu, and J. Li, "Development and experimental evaluation of a single-winding, dual-stator, spoke-array Vernier permanent magnet machines," in *Proc. IEEE Energy Convers. Congr. Expo. (ECCE)*, Sep. 2015, pp. 1885–1891.
[72] W. Liu and T. A. Lipo, "Alternating flux barrier design of Vernier ferrite magnet machine having high torque density," in *Proc. IEEE Electric Ship Technol. Symp. (ESTS)*, Aug. 2017, pp. 445–450.
[73] W. Liu and T. A. Lipo, "Analysis of consequent pole spoke type Vernier permanent magnet machine with alternating flux barrier design," *IEEE Trans. Ind. Appl.*, vol. 54, no. 6, pp. 5918–5929, Nov. 2018.
[74] X. Li, K. Tong Chau, and M. Cheng, "Comparative analysis and experimental verification of an effective permanent-magnet Vernier machine," *IEEE Trans. Magn.*, vol. 51, no. 7, pp. 1–9, Jul. 2015.
[75] Y. Gao, R. Qu, D. Li, J. Li, and G. Zhou, "Consequent-pole flux-reversal permanent-magnet machine for electric vehicle propulsion," *IEEE Trans. Appl. Supercond.*, vol. 26, no. 4, pp. 1–5, Jun. 2016.
[76] Z. Z. Wu and Z. Q. Zhu, "Partitioned stator flux reversal machine with consequent-pole PM stator," *IEEE Trans. Energy Convers.*, vol. 30, no. 4, pp. 1472–1482, Dec. 2015.
[77] H. Hua, Z. Q. Zhu, and H. Zhan, "Novel consequent-pole hybrid excited machine with separated excitation stator," *IEEE Trans. Ind. Electron.*, vol. 63, no. 8, pp. 4718–4728, Apr. 2016.
[78] B. Ren, G.-J. Li, Z. Q. Zhu, M. Foster, and D. A. Stone, "Performance comparison between consequent-pole and inset modular permanent magnet machines," *J. Eng.*, vol. 2019, pp. 3951–3955, Jul. 2018.
[79] S.-U. Chung, J.-W. Kim, B.-C. Woo, D.-K. Hong, J.-Y. Lee, and D.-H. Koo, "A novel design of modular three-phase permanent magnet Vernier machine with consequent pole rotor," *IEEE Trans. Magn.*, vol. 47, no. 10, pp. 4215–4218, Oct. 2011.
[80] A. Allahyari and H. Torkaman, "A novel high-performance consequent pole dual rotor permanent magnet Vernier machine," *IEEE Trans. Energy Convers.*, vol. 35, no. 3, pp. 1238–1246, Sep. 2020.
[81] D. K. Jang and J. H. Chang, "Design of a Vernier machine with PM on both sides of rotor and stator," *IEEE Trans. Magn.*, vol. 50, no. 2, pp. 877–880, Feb. 2014.
[82] W. Zhao, X. Sun, J. Ji, and G. Liu, "Design and analysis of new Vernier permanent-magnet machine with improved torque capability," *IEEE Trans. Appl. Supercond.*, vol. 26, no. 4, pp. 1–5, Jun. 2016.
[83] G. Xu, G. Liu, M. Chen, X. Du, and M. Xu, "Cost-effective Vernier permanent-magnet machine with high torque performance," *IEEE Trans. Magn.*, vol. 53, no. 11, pp. 1–4, Nov. 2017.
[84] K. Adnani, S. Shafiei, J. Millimonfared, and J. S. Moghani, "Modified unipolar hybrid permanent magnet Vernier machine using Halbach array configuration," in *Proc. 10th Int. Power Electron., Drive Syst. Technol. Conf. (PEDSTC)*, Feb. 2019, pp. 40–43.
[85] J. Huang, W. Fu, S. Niu, and X. Zhao, "Comparative analysis of different permanent magnet arrangements in a novel flux modulated electric machine," *IEEE Access*, vol. 9, pp. 14437–14445, 2021.
[86] D. K. Jang and J. H. Chang, "Performance comparison of PM synchronous and PM Vernier machines based on equal output power per unit volume," *J. Elect. Eng. Technol.*, vol. 11, no. 1, pp. 150–156, 2016.
[87] R. Ishikawa, K. Sato, S. Shimomura, and R. Nishimura, "Design of in-wheel permanent magnet Vernier machine to reduce the armature current density," in *Proc. Int. Conf. Electr. Mach. Syst. (ICEMS)*, Oct. 2013, pp. 459–464, doi: 10.1109/ICEMS.2013.6754567.
[88] K. Xie, D. Li, R. Qu, and Y. Gao, "A novel permanent magnet Vernier machine with Halbach array magnets in stator slot opening," *IEEE Trans. Magn.*, vol. 53, no. 6, pp. 1–5, Jun. 2017.
[89] Z. Liang, Y. Gao, D. Li, and R. Qu, "Design of a novel dual flux modulation machine with consequent-pole spoke-array permanent magnets in both stator and rotor," *CES Trans. Elect. Mach. Syst.*, vol. 2, no. 1, pp. 73–81, Mar. 2018.
[90] R. Hosoya and S. Shimomura, "Apply to in-wheel machine of permanent magnet Vernier machine using NdFeB bonded magnet—Fundamental study," in *Proc. 8th Int. Conf. Power Electron. (ECCE Asia)*, May/Jun. 2011, pp. 2208–2215.
[91] R. Hosoya, H. Shimada, and S. Shimomura, "Design of a ferrite magnet Vernier machine for an in-wheel machine," in *Proc. IEEE Energy Convers. Congr. Expo.*, Sep. 2011, pp. 2790–2797.
[92] Y. Tasaki, R. Hosoya, Y. Kashitani, and S. Shimomura, "Design of the Vernier machine with permanent magnets on both stator and rotor side," in *Proc. 7th Int. Power Electron. Motion Control Conf.*, Harbin, China, vol. 1, Jun. 2012, pp. 302–309.
[93] S. Kazuhiro, R. Hosoya, and S. Shimomura, "Design of NdFeB bond magnets for in-wheel permanent magnet Vernier machine," in *Proc. 15th Int. Conf. Elect. Mach. Syst. (ICEMS)*, Sapporo, Japan, Oct. 2012, pp. 21–24.
[94] K. Sato, R. Hosoya, and S. Shimomura, "Improved ferrite magnet Vernier machine for an in-wheel machine," in *Proc. IEEE Int. Conf. Power Energy (PECon)*, Kota Kinabalu, Malaysia, Dec. 2012, pp. 414–419.
[95] J. Li, K. T. Chau, J. Z. Jiang, C. Liu, and W. Li, "A new efficient permanent-magnet Vernier machine for wind power generation," *IEEE Trans. Magn.*, vol. 46, no. 6, pp. 1475–1478, Jun. 2010.
[96] X. Li, K. T. Chau, and M. Cheng, "Analysis, design and experimental verification of a field-modulated permanent-magnet machine for direct-drive wind turbines," *IET Electr. Power Appl.*, vol. 9, no. 2, pp. 150–159, 2015.
[97] Q. Wang, S. Niu, and T. W. Ching, "A new double-winding Vernier permanent magnet wind power generator for hybrid AC/DC microgrid application," *IEEE Trans. Magn.*, vol. 54, no. 11, pp. 1–5, Nov. 2018.
[98] B. Kim, "Design method of a direct-drive permanent magnet Vernier generator for a wind turbine system," *IEEE Trans. Ind. Appl.*, vol. 55, no. 5, pp. 4665–4675, Sep. 2019.
[99] M. M. Alavijeh and M. Mirsalim, "Design and optimization of a new dual-rotor Vernier machine for wind-turbine application," in *Proc. 28th Iranian Conf. Electr. Eng. (ICEE)*, Tabriz, Iran, Aug. 2020, pp. 1–6.
[100] J. Yu, C. Liu, and H. Zhao, "Design and multi-mode operation of double-stator toroidal-winding PM Vernier machine for wind-photovoltaic hybrid generation system," *IEEE Trans. Magn.*, vol. 55, no. 7, pp. 1–7, Jul. 2019.
[101] H. Polinder, D. Bang, R. P. J. O. M. van Rooij, A. S. McDonald, and M. A. Mueller, "10 MW wind turbine direct-drive generator design with pitch or active speed stall control," in *Proc. IEEE Int. Electr. Mach. Drives Conf.*, May 2007, pp. 1390–1395.
[102] Y. Gao, R. Qu, J. Li, Z. Zhu, and D. Li, "HTS Vernier machine for direct-drive wind power generation," *IEEE Trans. Appl. Supercond.*, vol. 24, no. 5, pp. 1–5, Oct. 2014.

DILEEP KUMAR KANA PADINHARU received the B.Tech. degree in electrical and electronics engineering from the College of Engineering Trivandrum, Kerala, India, in 2004, and the M.Sc. degree in high-voltage engineering from the Indian Institute of Science Bangalore, India, in 2007. He is currently pursuing the Ph.D. degree in electrical engineering with The University of Sheffield, U.K. He worked for General Electric Company, India, from 2007 to 2017, where he was involved in designing high-power synchronous generators. His research interests include the design, modeling, and optimization of permanent magnet machines.

GUANG-JIN Li (Senior Member, IEEE) received the bachelor's degree from Wuhan University, China, in 2007, the master's degree from the University of Paris XI, France, in 2008, and the Ph.D. degree from the Ecole Normale Supérieure (ENS) de Cachan, Paris, France, in 2011, all in electrical and electronic engineering. He joined the Electrical Machines and Drives (EMD) Group, The University of Sheffield, Sheffield, U.K., in June 2012, as a Postdoctoral Research Associate, where he was appointed as an Assistant Professor, in September 2013, and promoted as an Associate Professor, in January 2018, and a Professor, in January 2022. His main research interests include the design, fault diagnostics, and thermal management of electrical machines for renewable energy, automotive, and electrical aircrafts.

ZI-QIANG ZHU (Fellow, IEEE) received the B.Eng. and M.Sc. degrees in electrical and electronic engineering from Zhejiang University, Hangzhou, China, in 1982 and 1984, respectively, and the Ph.D. degree in electronic and electrical engineering from The University of Sheffield, Sheffield, U.K., in 1991. Since 1988, he has been with The University of Sheffield, where he currently holds the Royal Academy of Engineering/Siemens Research Chair and is the Head of the Electrical Machines and Drives Research Group, the Academic Director of the Sheffield Siemens Gamesa Renewable Energy Research Centre, the Director of the CRRC Electric Drives Technology Research Centre, and the Director of Midea the Electric Machines and Controls Research Centre. His research interests include the design and control of permanent-magnet brushless machines and drives for applications ranging from automotive through domestic appliances to renewable energy. He is a Fellow of the Royal Academy of Engineering.

RICHARD CLARK received the B.Eng. degree in electrical engineering from The University of Sheffield and the Ph.D. degree in permanent magnet actuators, in 1999. Following several years as a Postdoctoral Research Associate, he became a Lecturer in electrical engineering at The University of Sheffield, in 2005. In 2007, he joined Magnomatics—a University of Sheffield spin-out company developing novel electrical motors and generators and magnetic transmissions, where he held posts of a Research and Development Manager, the Research Director, and the Principal Engineer. He joined Siemens Gamesa Renewable Energy Research Centre, Sheffield, U.K., as an Electromagnetic Specialist, in October 2017.

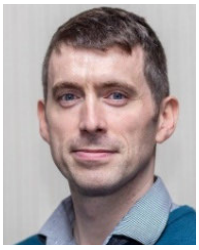

ARWYN THOMAS received the M.Eng. and Ph.D. degrees in electronic and electrical engineering from The University of Sheffield, Sheffield, U.K., in 2005 and 2009, respectively. He is currently with the Sheffield Siemens Gamesa Renewable Energy Research Centre, Sheffield, U.K. His research interest includes modeling, design, and analysis of permanent-magnet brushless machines.

ZIAD AZAR received the B.Eng. degree in electrical engineering from the University of Damascus, Damascus, Syria, in 2003, and the M.Sc. degree in electronic and electrical engineering and the Ph.D. degree in electrical engineering from The University of Sheffield, Sheffield, U.K., in 2008 and 2012, respectively. In 2012, he joined Siemens Games Renewable Energy Ltd., where he is currently the Generator Team Manager with the Technology Development Department, with a focus on maturing and developing new technologies for direct-drive wind power generators. His major research interests include the modeling, design, and analysis of permanent-magnet and magnetless brushless machines for automotive applications.

ALEXANDER DUKE received the M.Eng. and Ph.D. degrees in electrical engineering from The University of Sheffield, U.K., in 2011 and 2015, respectively. Since 2016, he has been with Siemens Gamesa Renewable Energy Research Centre, where he is currently an Advanced Engineer specializing in the electromagnetic design of permanent magnet wind power generators.